THE JOURNAL OF PHYSICAL CHEMISTRY B

ARTICLE

pubs.acs.org/JPCB

Electric-Field-Induced Changes in Absorption and Fluorescence of the Green Fluorescent Protein Chromophore in a PMMA Film

Takakazu Nakabayashi,*[,†] Kazuyuki Hino,[‡] Yuka Ohta,[‡] Sayuri Ito,[‡] Hirofumi Nakano,[‡] and Nobuhiro Ohta*[,†]

[†]Research Institute for Electronic Science (RIES), Hokkaido University, Sapporo 001-0020, Japan

[‡]Department of Chemistry, Aichi University of Education, Hirosawa 1, Igaya, Kariya 448-8542, Japan

ABSTRACT: External electric field effects on absorption, fluorescence, and fluorescence decay of *p*-HBDI that is a model compound of the chromophore of GFP have been examined in a poly(methyl methacrylate) film. The electroabsorption spectrum is similar in shape to the first derivative of the absorption spectrum, which results from the difference in molecular polarizability between the ground state and the Franck−Condon excited state. The electrophotoluminescence spectrum is dominated by the corresponding fluorescence spectrum, indicating the enhancement of the fluorescence intensity in the presence of external electric fields. The direct measurements of the electric field effect on the fluorescence decay profile suggest that the field-induced deceleration of the nonradiative process contributes to the increase in the fluorescence intensity in the presence of electric fields.

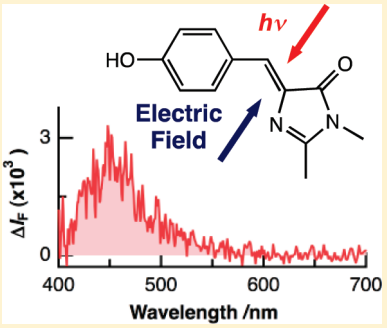

1. INTRODUCTION

The green fluorescent protein (GFP) from the jellyfish *Aequorea victoria* has been widely used as a fluorescent marker in molecular and cell biology.[1,2] Many different mutants of GFP have been engineered to add useful photophysical characters such as shifted fluorescence wavelength and enhanced fluorescence intensity.[3,4] The chromophore of GFP exhibiting absorption and fluorescence in the visible region consists of a structure of *p*-hydroxybenzylidene-imidazolidinone (*p*-HBI), which is rigidly encapsulated inside a can-shaped tertiary structure created by an eleven β-strands in a single polypeptide.[5,6] The large steric hindrance due to the protein structure interferes with the nonradiative relaxation of the chromophore, resulting in the increase in the fluorescence quantum yield: the fluorescence quantum yield of the native protein is 0.8, while that of the synthetic GFP chromophore is $<10^{-3}$ in fluid solutions.[2,3,7]

The protein environment surrounding the chromophore is also responsible for optical properties of GFP. The GFP chromophore is surrounded by both apolar and polar residues of a single polypeptide and these charged residues produce a strong electric field for the embedded chromophore.[5,6,8] It has been reported that charged and polar groups within a protein structure produce an electric field of 1 to 80 MV cm^{-1} for embedded molecules.[9−11] However, effects of electric fields on the photoexcitation dynamics of the GFP chromophore remain unclear. Systematic studies on field-induced changes in photophysical properties of the fluorescent chromophore are very important for optimizing GFP mutants for specific applications.

In the present study, external electric field effects on the photoexcitation dynamics of the synthetic model chromophore of GFP have been investigated using electric field modulation spectroscopy.[12−14] We have prepared a poly(methyl methacrylate) (PMMA) film in which the model chromophore is isotropically distributed, and field-induced changes in its absorption and fluorescence spectra (electroabsorption and electrophotoluminescence spectra, respectively) and fluorescence decay have been measured. We have used a dimethyl derivative of *p*-HBI (*p*-HBDI) that can be regarded as a model chromophore of wild-type GFP and several GFP mutants such as EGFP and EYFP.[2,3,15−24] *p*-HBDI exists as a mixture of *Z* and *E* isomers (Scheme 1) in solution phases.[20,24−26] Hereafter, electroabsorption and electrophotoluminescence spectra are abbreviated as E-A and E-PL spectra, respectively, and applied electric field is denoted by ***F***. All the measurements were performed at room temperature.

2. EXPERIMENTAL SECTION

p-HBDI was synthesized according to the literature methods.[27,28] Briefly, glycine was reacted with 4-hydroxybenzaldehyde and sodium acetate in acetic anhydride. The generated azlactone was then treated with methylamine in the presence of K_2CO_3. *p*-HBDI was purified by sublimation and recrystallization from ethanol. ESI-MS analyses (positive and negative ion modes) gave $m/z = 217\ [M + 1]^+$ and $215\ [M - 1]^-$, respectively. The spin-coated PMMA film was prepared on an indium-tin-oxide (ITO)-coated quartz substrate. Then 2.5 ml of chloroform solution-containing PMMA (50 mg) was mixed with 0.4 mL of ethanol solution containing *p*-HBDI (ca. 1 mg), and the obtained mixture of *p*-HBDI and PMMA was cast on the first-prepared PMMA film by spin coating. The concentration of *p*-HBDI was ca. 1 mol % in its ratio to the monomer unit of PMMA. A

Received: April 3, 2011
Revised: May 26, 2011
Published: June 03, 2011

Scheme 1. *Z* and *E* Isomers of *p*-HBDI

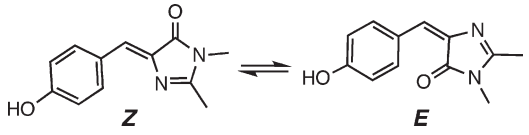

semitransparent aluminum film was deposited on the polymer film by vacuum vapor deposition. The ITO and aluminum films were used as electrodes.

E-A and E-PL spectra were measured using electric field modulation spectroscopy with the same apparatus as previously reported.[12,13] A sinusoidal ac voltage was applied to a sample with a modulation frequency of 40 Hz. Field-induced change in absorption intensity or fluorescence intensity was detected with a lock-in amplifier at the second harmonic of the modulation frequency. A dc component of the transmitted light intensity or the fluorescence intensity was simultaneously observed. E-A and E-PL spectra were obtained by plotting the change in absorption intensity and in fluorescence intensity as a function of wavenumber, respectively. Applied field strength was evaluated from the applied voltage divided by the film thickness. The angle between the direction of the applied electric field and the electric vector of the excitation light was set to be 54.7° (magic angle) in the E-A measurements, and depolarized emission was detected in the E-PL measurements.

Measurements of the field-induced change in fluorescence decay were carried out using a single-photon counting system combined with a pulse generator supplying a bipolar square wave.[14] The second harmonic of the output from a femtosecond mode-locked Ti:sapphire laser (Spectra Physics, Tsunami) was used for the excitation, and the repetition rate of the laser pulse was reduced with a pulse picker (model 350-160, Conoptics) to ca. 6 MHz from the original 81 MHz. Fluorescence passed through a color glass filter and a monochromator (Nikon, G-250) was detected with a microchannel-plate photomultiplier (Hamamatsu, R3809U-52). Fluorescence signal was amplified, discriminated, and then led to a time-to-amplitude converter system. Fluorescence decays were measured by a multichannel pulse height analyzer (SEIKO EG&G, model 7700). The instrumental response function (IRF) had a pulse width of ca. 60 ps (FWHM). The observed fluorescence decay was fitted by the convolution of the IRF with a multiexponential decay function. The minimum lifetime that could be distinguished in the present analysis was ca. 10 ps.[14] Applied voltage was a repetition of rectangular waves of positive, zero, negative, and zero bias. The time duration of each bias was 30 ms, but the first 2 ms was a deadtime to exclude an overshooting of the applied field. Four different decays were collected, corresponding to positive, zero, negative, and zero sample bias. These decays were stored in each of the different memory-segments of the multichannel pulse height analyzer.

3. RESULTS AND DISCUSSION

Figure 1 shows the E-A spectrum of *p*-HBDI in a PMMA film with a field strength of 0.7 MV cm^{-1}, together with the absorption spectrum. The absorption spectrum in PMMA was similar to that in solution phases[16,19,20,25] and the absorption band with a peak at ca. 372 nm can be assigned to the transition to

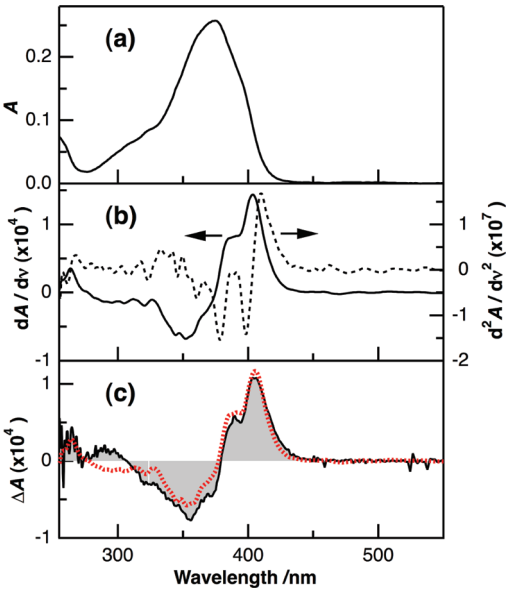

Figure 1. (a) Absorption spectrum of *p*-HBDI in a PMMA film, (b) the first (solid line) and second (dotted line) derivative spectra of the above absorption spectrum, (c) E-A spectrum (shaded line) and the fitted one (dotted line). The applied field strength was 0.7 MV cm^{-1}.

the first excited $2^1A'$ state of the neutral form of *p*-HBDI.[29] The first and second derivatives of the absorption spectrum are also shown in this figure. The field-induced change in absorption intensity of an isotropic sample at wavenumber ν, that is, $\Delta A(\nu)$, in rigid matrices such as PMMA, is given by a sum of the zeroth, first, and second derivatives of the absorption $A(\nu)$ as follows[30−32]

$$\Delta A(\nu) = (fF)^2 \left[A'A(\nu) + B'\nu \frac{d\left\{\frac{A(\nu)}{\nu}\right\}}{d\nu} + C'\nu \frac{d^2\left\{\frac{A(\nu)}{\nu}\right\}}{d\nu^2} \right] \quad (1)$$

where f is the internal field factor. The coefficient A' depends on the transition polarizability. B' and C' correspond to the spectral shift and spectral broadening resulting from the differences in molecular polarizability ($\Delta\boldsymbol{\alpha}$) and in electric dipole moment ($\Delta\boldsymbol{\mu}$), respectively, between the ground state and the excited state, which are given as follows

$$B' = \frac{\frac{\Delta\bar{\alpha}}{2} + \frac{(\Delta\alpha_m - \Delta\bar{\alpha})(3\cos^2\chi - 1)}{10}}{hc} \quad (2)$$

$$C' = |\Delta\boldsymbol{\mu}|^2 \frac{[5 + (3\cos^2\xi - 1)(3\cos^2\chi - 1)]}{30h^2c^2} \quad (3)$$

where $\Delta\bar{\alpha}$ denotes the trace of $\Delta\alpha$; $\Delta\alpha_m$ is the diagonal component of $\Delta\boldsymbol{\alpha}$ with respect to the direction of the transition dipole moment; χ is the angle between the direction of $\boldsymbol{F}$ and the electric vector of the light; and ξ is the angle between the direction of $\Delta\boldsymbol{\mu}$ and the transition dipole moment. The magic angle condition of $\chi = 54.7°$ was used in Figure 1c.

The magnitude of the field-induced change in absorption intensity was proportional to the square of applied field strength, as expected from eq 1 (Figure 2a). The observed E-A spectrum

dx.doi.org/10.1021/jp203090e |*J. Phys. Chem. B* 2011, 115, 8622–8626

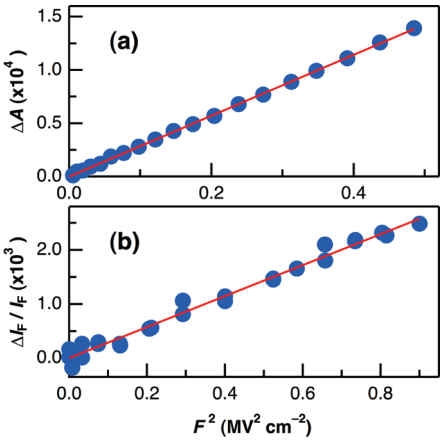

Figure 2. Plots of the field-induced change in absorption intensity (a) and in fluorescence intensity (b) of *p*-HBDI in a PMMA film as a function of the square of applied field strength. The fitted line is shown in each panel by a solid line. The observed absorption and fluorescence wavelengths were 405 and 450 nm, respectively.

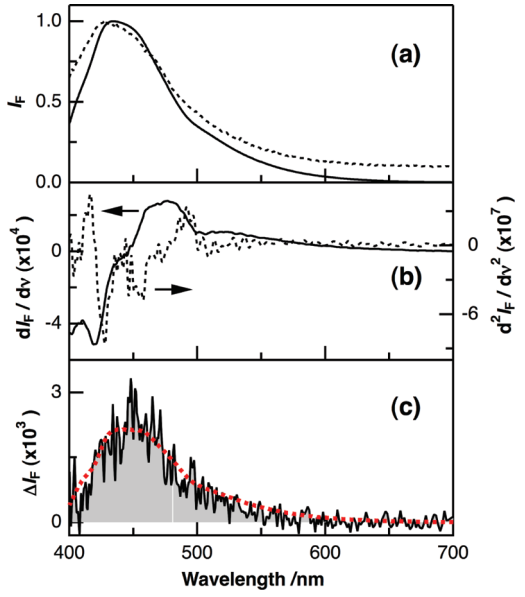

Figure 3. (a) Fluorescence spectra of *p*-HBDI in a PMMA film with the excitation wavelengths of 370 nm (solid line) and 379 nm (dotted line), (b) the first (solid line) and second (dotted line) derivative spectra of the fluorescence spectrum at the 370-nm excitation wavelength, (c) E-PL spectrum (shaded line) and the fitted one (dotted line). Excitation wavelength for the E-PL measurement was 379 nm. The applied field strength was 0.9 MV cm^{-1}.

was similar in shape to the first derivative of the corresponding absorption spectrum, although a small contribution of both absorption spectrum and its second derivative was necessary to fit the E-A spectrum, as shown in Figure 1c. From the coefficients of the first and second derivative spectra, the $\Delta\bar{\alpha}$ and $|\Delta\boldsymbol{\mu}|$ values between the Franck−Condon (FC) excited state and the ground state of the neutral form of *p*-HBDI were evaluated to be ca. 70 Å^3 and 2 D, respectively, by assuming that the local field was the same as the applied field, that is, $f = 1$ in eq 1. The obtained small difference in electric dipole moment between the FC and ground states is consistent with the theoretical calculation.[29]

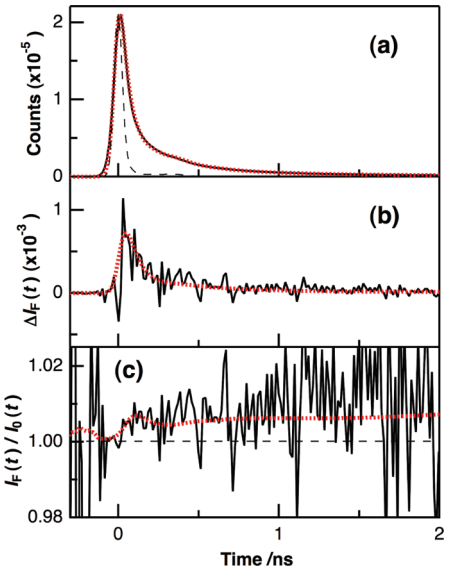

Figure 4. (a) Representative fluorescence decay (solid line) of *p*-HBDI in a PMMA film at zero field, (b) the difference between the decays at 1.1 MV cm^{-1} and at zero field (solid line), (c) the ratio of the decay at 1.1 MV cm^{-1} relative to that at zero field (solid line). The fitted curve is shown in each panel by a dotted line. The fluorescence decay in ethanol is also shown in (a) by a dashed line. Excitation and monitoring wavelengths were 379 and 450 nm, respectively.

Figure 3 shows the fluorescence and E-PL spectra of *p*-HBDI in a PMMA film. Excitation wavelength for the E-PL measurement was 379 nm, where the field-induced change in absorption intensity was negligibly small. Applied field strength was 0.9 MV cm^{-1}. The fluorescence arises from the neutral form of *p*-HBDI.[16,19] The magnitude of the field-induced change in fluorescence intensity was proportional to the square of applied field strength (Figure 2b). In contrast to the E-A spectrum, it was found from the E-PL spectrum that the fluorescence of *p*-HBDI in PMMA was markedly enhanced in the presence of ***F***. The dominance of the field-induced fluorescence enhancement in the E-PL spectrum was also confirmed at the excitation wavelength of 307 nm, where the field-induced change in absorption intensity was also very small (Figure 1c). The E-PL spectrum was fitted by a superposition of the fluorescence spectrum and its first derivative spectrum (Figure 3c). The fluorescence spectrum obtained with the 370 nm excitation wavelength was used for the simulation in Figure 3 because the scattered light was overlapped with the fluorescence spectrum with excitation at 379 nm. It is noted that the scattered light was not affected by the application of electric fields. The zeroth derivative component in the E-PL spectrum indicates the field-induced enhancement of the fluorescence, as in the case of porphyrin-C_{60} dyads.[33] The magnitude of the enhancement of the fluorescence was ca. 0.2% with a field strength of 0.9 MV cm^{-1}.

From the steady state measurements, it is difficult to confirm whether the field-induced enhancement of the fluorescence intensity is due to a change in fluorescence lifetime or a change in initial population of the fluorescent state. To elucidate the mechanism of field effects on the photoexcitation dynamics, therefore, we have measured electric field effects on the fluorescence decay profile of *p*-HBDI.[14] Figure 4a shows the fluorescence decay of *p*-HBDI in PMMA in the absence of ***F***. Excitation and monitoring wavelengths were 379 and 450 nm, respectively.

The fluorescence decay of *p*-HBDI in ethanol is also shown in this figure. The fluorescence lifetime of *p*-HBDI in ethanol was reported to be in the subpicosecond range at room temperature,[16,18] which is much shorter than the FWHM of the IRF. In fact, the same shape as the response function was observed for the decay profile of *p*-HBDI in ethanol. However, the fluorescence in PMMA exhibited a multiexponential decay; the fluorescence lifetime of the major component was ca. 40 ps, and the minor decaying components having fluorescence lifetimes of ca. 260 ps and 1.2 ns were also confirmed. The increase of the fluorescence lifetime in PMMA may arise from the deenhancement of the nonradiative transition caused by the steric hindrance of *p*-HBDI in the polymer film. Such a lengthening of the fluorescence lifetime in PMMA has also been observed for a derivative of *p*-HBDI in which methyl groups are replaced by phenyl groups: the average fluorescence lifetime in ethanol was 1.6 ps and that in PMMA was 1.7 ns.[34]

The difference between the decays observed at zero field ($I_0(t)$) and at 1.1 MV cm^{-1} ($I_F(t)$), that is, $I_F(t) - I_0(t)$, referred to as $\Delta I_F(t)$, and the ratio $I_F(t)/I_0(t)$ are shown in Figure 4b,c, respectively. The time integration of $\Delta I_F(t)$ in Figure 4b was positive, showing that the fluorescence intensity was enhanced by ***F***, which is in agreement with the one obtained from the E-PL spectrum. If the fluorescence lifetime is independent of ***F***, the intensity ratio between the two decays with and without ***F*** would remain constant over the whole time region. In Figure 4c, the value of $I_F(t)/I_0(t)$ was not constant during the decay but increased with a passage of time in the 0−200 ps region, suggesting that the fluorescence lifetime becomes longer in the presence of ***F***. The field-induced increase in the fluorescence lifetime is expected when the nonradiative decay rate is decreased by ***F***. The time profiles of $\Delta I_F(t)$ and $I_F(t)/I_0(t)$ are very sensitive to the changes in the parameters of the decay. By simulating these time profiles, the magnitude of the small changes in the lifetime and in the preexponential factor could be evaluated.[14,22,35] As shown in Figure 4, all the time profiles of $I_0(t)$, $I_F(t)$, $\Delta I_F(t)$, and $I_F(t)/I_0(t)$ were fitted by assuming a triexponential decay, that is, $\Sigma_i A_i \exp(-t/\tau_i)$, where A_i and τ_i denote the pre-exponential factor and lifetime of component *i*, respectively. The lifetime and the preexponential factor of each component used in Figure 4 were as follows: $\tau_1 = 43$ ps, $\tau_2 = 260$ ps, $\tau_3 = 1210$ ps, $A_1 = 0.896$, $A_2 = 0.089$, $A_3 = 0.015$ in the absence of ***F***, and $\tau_1 = 44$ ps, $\tau_2 = 261$ ps, $\tau_3 = 1215$ ps, $A_1 = 0.895$, $A_2 = 0.089$, $A_3 = 0.015$ in the presence of 1.1 MV cm^{-1}. The sum of the preexponential factors in the absence of ***F*** was normalized to unity in this evaluation. The average fluorescence lifetime, defined by $\Sigma_i A_i \tau_i / \Sigma_i A_i$, was evaluated to be 80 ps at zero field and 81 ps at 1.1 MV cm^{-1}. This result suggests that the lengthening of the fluorescence lifetime in the presence of ***F***, which can be attributed to the field-induced deceleration of the nonradiative process of the fluorescent state of *p*-HBDI, contributes to the field-induced enhancement of the fluorescence in Figure 3. The time integration of fluorescence decay profile with the normalized intensity allows us to estimate the change in fluorescence yield arising from fluorescence lifetime. In the time range up to 3 ns, the ratio of the integrated value of the normalized intensity in the presence to that in the absence of 1.1 MV cm^{-1} is ca. 0.5%, which is comparable in magnitude with the intensity change of ca. 0.2% at 0.9 MV cm^{-1} (Figure 3). The similar magnitudes of the field-induced changes in the fluorescence lifetime and in the fluorescence intensity support the present conclusion.

As mentioned in Introduction, the magnitude of the electric field in a protein structure has been reported to be 1−80 MV cm^{-1} for bounded molecules such as carbon monoxide in myoglobin.[9−11] The magnitude of the electric field produced by the protein structure is therefore considered to be much larger than the applied field used in the present study. Furthermore, the magnitude of the field-induced change is proportional to the square of applied field strength, as is shown in Figure 2. From these results, it can therefore be said that the strength of the electric field produced by charged and polar groups within the protein is one of the key factors affecting the photoexcitation dynamics of *p*-HBI in GFP.

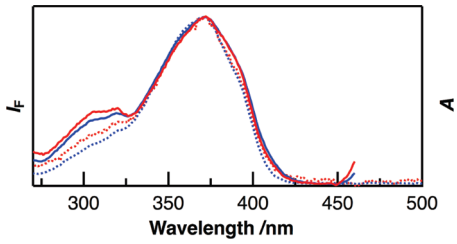

Figure 5. Representative excitation spectra (solid line) and absorption spectra (dotted line) of *p*-HBDI in a PMMA film. The concentration in the ratio to the monomer unit of PMMA was ca. 1 mol % (blue) and ca. 0.2 mol % (red). The maximum intensities of all the spectra are normalized to unity. Fluorescence at 480 nm was monitored for the measurements of the excitation spectra.

As mentioned above, *p*-HBDI in PMMA showed a multiexponential fluorescence decay, which probably arises from inhomogeneous environments in a polymer film, that is, the presence of different interactions between *p*-HBDI and PMMA which give different fluorescence lifetimes from each other.[35] It should be noted that the fluorescence excitation spectrum of *p*-HBDI did not coincide with the absorption spectrum in PMMA (Figure 5). The absorption spectrum in PMMA was similar to that of the *Z*-isomer of *p*-HBDI that is known to be more stable than the *E*-isomer in fluid solutions.[16,19,20,25] On the other hand, the excitation spectrum in PMMA was similar in shape to the reported absorption spectrum of the *E*-isomer of *p*-HBDI;[20,25] the structured excitation band around 320 nm is observed in the absorption spectrum of the *E*-isomer. It is noted that the excitation band around 320 nm was observed irrespective of the monitoring fluorescence wavelengths of 450, 480, and 515 nm. This result suggests that not only the *Z*-isomer but also the *E*-isomer of *p*-HBDI contributes to the observed fluorescence in PMMA. The structured excitation band does not arise from aggregates of *p*-HBDI because the same excitation spectrum was observed at a lower concentration of ca. 0.2 mol % (Figure 5). The excitation energy transfer from impurities of PMMA[17] to *p*-HBDI can also be neglected because the excitation band in the 290−330 nm region was not observed in the excitation spectrum of impurities of PMMA exhibiting very weak emission. It has been reported that the thermal isomerization from the *E* to *Z* isomers is faster in water than in methanol or isopropanol, suggesting that the polarity of water stabilizes the transition state for the ground state isomerization.[24] The thermal *E* to *Z* isomerization has also been shown to become very slow in aprotic solvents.[26] It is therefore conceivable that the *E*-isomer is comparatively stabilized in PMMA due to weak polar and/or aprotic character of PMMA.

The present study suggests the field-induced deceleration of the nonradiative transition of the neutral form of *p*-HBDI in a PMMA film. The NMR study on the photoisomerization of *para*-amino analogue of HBDI suggests that the main nonradiative

pathway of the *Z*-form of *p*-HBDI in aprotic solvents is the formation of the twisted intermediate around the C═C bond, resulting in the formation of the *E*-isomer.[26] It is expected that the C═C bond twisted intermediate is also formed following excitation of the *E*-isomer as in the case of *trans*−*cis* photoisomerization of stilbenes.[36] Since the rate of charge transfer (CT) of a molecule and molecular systems is affected by $\boldsymbol{F}$,[32] the present result suggests that the twisted intermediate of the conformational relaxation of *p*-HBDI has a CT character. In our previous study, the fluorescence lifetime of GFPuv5, which is a UV-excited GFP variant, was observed in a poly(vinyl alcohol) film (PVA) to become shorter in the presence of $\boldsymbol{F}$.[22] Although GFPuv5 was not in the native conformation in PVA, that observation suggested that the nonradiative transition of the anionic chromophore was accelerated by $\boldsymbol{F}$. Comparison of the field effects on the fluorescence both of the neutral form and of the anionic form of *p*-HBDI may be important as a future program.

4. CONCLUSIONS

External electric field effects on the absorption and fluorescence spectra and the fluorescence decay of the neutral form of *p*-HBDI have been investigated in a PMMA film. The E-A spectrum was similar in shape to the first derivative of the absorption spectrum and the differences in molecular polarizability and in electric dipole moment between the ground state and the Franck−Condon excited state were evaluated. It was found from the E-PL spectrum that the fluorescence of *p*-HBDI was enhanced in the presence of external electric fields. The measurements of the field-induced change in the fluorescence decay profile suggested that the field-induced deceleration of the nonradiative process contributes to the observed field-induced increase in the fluorescence intensity. It is therefore important to consider the strength of the local electric field when discussing the nonradiative transition of the neutral chromophore within the protein structure. The excitation spectrum of *p*-HBDI in PMMA was similar in shape to the absorption spectrum of its *E*-isomer, suggesting that the *E*-isomer was comparatively stabilized in PMMA. Finally, it is hoped that the present results would be useful not only for understanding the photochemistry of the chromophore of GFP but also for optimizing optical properties of GFP mutants for specific applications.

AUTHOR INFORMATION

Corresponding Author

*(T.N.) E-mail: takan@es.hokudai.ac.jp. Phone: +81-11-706-9407. (N.O.) E-mail: nohta@es.hokudai.ac.jp. Phone: +81-11-706-9410.

ACKNOWLEDGMENT

This work has been supported in part by Grants-in-Aid for Scientific Research (Grant Nos. 22350031 and 20245001) from the Ministry of Education, Culture, Sports, Science, and Technology (MEXT) and Japan Society for the Promotion of Science (JSPS) in Japan.

REFERENCES

(1) Shimomura, O.; Johnson, F. H.; Saiga, Y. *J. Cell. Comp. Physiol.* **1962**, *59*, 223–239.
(2) Tsien, R. Y. *Annu. Rev. Biochem.* **1998**, *67*, 509–544.
(3) Zimmer, M. *Chem. Rev.* **2002**, *102*, 759–781.
(4) Shaner, N. C.; Steinbach, P. A.; Tsien, R. Y. *Nat. Methods* **2005**, *2*, 905–909.
(5) Ormö, M.; Cubitt, A. B.; Kallio, K.; Gross, L. A.; Tsien, R. Y.; Remington, S. J. *Science* **1996**, *273*, 1392–1395.
(6) Yang, F.; Moss, L. G.; Phillips, G. N., Jr. *Nat. Biotechnol.* **1996**, *14*, 1246–1251.
(7) Niwa, H.; Inouye, S.; Hirano, T.; Matsuno, T.; Kojima, S.; Kubota, M.; Ohashi, M.; Tsuji, F. I. *Proc. Natl. Acad. Sci. U.S.A.* **1996**, *93*, 13617–13622.
(8) Brejc, K.; Sixma, T. K.; Kitts, P. A.; Kain, S. R.; Tsien, R. Y.; Ormö, M.; Remington, S. J. *Proc. Natl. Acad. Sci. U.S.A.* **1997**, *94*, 2306–2311.
(9) Callis, P. R.; Burgess, B. K. *J. Phys. Chem. B* **1997**, *101*, 9429–9432.
(10) Park, E. S.; Andrews, S. S.; Hu, R. B.; Boxer, S. G. *J. Phys. Chem. B* **1999**, *103*, 9813–9817.
(11) Kriegl, J. M.; Nienhaus, K.; Deng, P.; Fuchs, J.; Nienhaus, G. U. *Proc. Natl. Acad. Sci. U.S.A.* **2003**, *100*, 7069–7074.
(12) Ohta, N.; Koizumi, M.; Umeuchi, S.; Nishimura, Y.; Yamazaki, I. *J. Phys. Chem.* **1996**, *100*, 16466–16471.
(13) Ohta, N.; Umeuchi, S.; Nishimura, Y.; Yamazaki, I. *J. Phys. Chem. B* **1998**, *102*, 3784–3790.
(14) Tsushima, M.; Ushizaka, T.; Ohta, N. *Rev. Sci. Instrum.* **2004**, *75*, 479–485.
(15) Weber, W.; Helms, V.; McCammon, J. A.; Langhoff, P. W. *Proc. Natl. Acad. Sci. U.S.A.* **1999**, *96*, 6177–6182.
(16) Kummer, A. D.; Kompa, C.; Niwa, H.; Hirano, T.; Kojima, S.; Michel-Beyerle, M. E. *J. Phys. Chem. B* **2002**, *106*, 7554–7559.
(17) Litvinenko, K. L.; Webber, N. M.; Meech, S. R. *J. Phys. Chem. A* **2003**, *107*, 2616–2623.
(18) Mandal, D.; Tahara, T.; Meech, S. R. *J. Phys. Chem. B* **2004**, *108*, 1102–1108.
(19) Solntsev, K. M.; Poizat, O.; Dong, J.; Rehault, J.; Lou, Y.; Burda, C.; Tolbert, L. M. *J. Phys. Chem. B* **2008**, *112*, 2700–2711.
(20) Voliani, V.; Bizzarri, R.; Nifosi, R.; Abbruzzetti, S.; Grandi, E.; Viappiani, C.; Beltram, F. *J. Phys. Chem. B* **2008**, *112*, 10714–10722.
(21) Olsen, S.; Smith, S. C. *J. Am. Chem. Soc.* **2008**, *130*, 8677–8689.
(22) Nakabayashi, T.; Kinjo, M.; Ohta, N. *Chem. Phys. Lett.* **2008**, *457*, 408–412.
(23) Meech, S. R. *Chem. Soc. Rev.* **2009**, *38*, 2922–2934.
(24) He, X.; Bell, A. F.; Tonge, P. J. *FEBS Lett.* **2003**, *549*, 35–38.
(25) Dong, J.; Abulwerdi, F.; Baldridge, A.; Kowalik, J.; Solntsev, K. M.; Tolbert, L. M. *J. Am. Chem. Soc.* **2008**, *130*, 14096–14098.
(26) Yang, J.-S.; Huang, G.-J; Liu, Y.-H.; Peng, S.-M. *Chem. Commun.* **2008**, 1344–1346.
(27) Kojima, S.; Ohkawa, H.; Hirano, T.; Maki, S.; Niwa, H.; Ohashi, M.; Inouye, S.; Tsuji, F. I. *Tetrahedron Lett.* **1998**, *39*, 5239–5242.
(28) He, X.; Bell, A. F.; Tonge, P. J. *Org. Lett.* **2002**, *4*, 1523–1526.
(29) Das, A. K.; Hasegawa, J.-Y.; Miyahara, T.; Ehara, M.; Nakatsuji, H. *J. Comput. Chem.* **2003**, *24*, 1421–1431.
(30) Bublitz, G. U.; Boxer, S. G. *Annu. Rev. Phys. Chem.* **1997**, *48*, 213–242.
(31) Locknar, S. A.; Peteanu, L. A. *J. Phys. Chem. B* **1998**, *102*, 4240–4246.
(32) Ohta, N. *Bull. Chem. Soc. Jpn.* **2002**, *75*, 1637–1655.
(33) Ohta, N.; Mikami, S.; Iwaki, Y.; Tsushima, M.; Imahori, H.; Tamaki, K.; Sakata, Y.; Fukuzumi, S. *Chem. Phys. Lett.* **2003**, *368*, 230–235.
(34) Petkova, I.; Dobrikov, G.; Banerji, N.; Duvanel, G.; Perez, R.; Dimitrov, V.; Nikolov, P.; Vauthey, E. *J. Phys. Chem. A* **2010**, *114*, 10–20.
(35) Nakabayashi, T.; Wahadoszamen, Md.; Ohta, N. *J. Am. Chem. Soc.* **2005**, *127*, 7041–7052.
(36) Waldeck, D. H. *Chem. Rev.* **1991**, *91*, 415–436.